arXiv:1605.00541v1 [physics.ao-ph] 2 May 2016

Higher-order approximations of the residual-mean eddy streamfunction and the quasi-Stokes streamfunction

Jan Viebahn * and Carsten Eden

KlimaCampus, University Hamburg, Hamburg, Germany

May 3, 2016

Abstract

The series expansion of the residual-mean eddy streamfunction and the quasi-Stokes streamfunction are compared up to third order in buoyancy perturbation, both formally and by using several idealised eddy-permitting zonal channel model experiments. In model configurations with flat bottom, both streamfunctions may be well approximated by the first one or two leading order terms in the ocean interior, although terms up to third order still significantly impact the implied interior circulations. Further, differences in both series expansions up to third order remain small here. Near surface and bottom boundaries, on the other hand, the leading order terms differ and are initially of alternating sign and of increasing magnitude such that the low order approximate expressions break down there. In more realistic model configurations with significant topographic features, physically inconsistent recirculation cells also appear in the ocean interior and are not effectively reduced by the next higher order terms. A measure indicating an initially increasing or decreasing series expansion is proposed.

* *Corresponding author address:* Jan Viebahn, KlimaCampus, Institute of Oceanography, University of Hamburg, Bundesstraße 53, 20146 Hamburg, Germany.
E-mail: jan.viebahn@zmaw.de. Tel/fax: +49 40 42838 -8215/-2995.

1 Introduction

Eulerian averaging of velocities and tracers is usually considered as the simplest way of averaging: Time and ensemble averages are performed at fixed position and space averages are solely defined by the geometrical framework (i.e. by the coordinate lines of the geometrically natural coordinate system). In other words, Eulerian averaging appears to be the most straightforward averaging procedure, because no physical properties of the fluid are taken into account in the integration conditions (Andrews and McIntyre, 1978a). Accordingly, the Eulerian meridional transport streamfunction Λ, i.e. the zonally integrated meridional transport of fluid across a given latitude y and below a constant height surface z, is defined in regard to the space coordinates y and z.

However, Λ gives rise to spurious diabatic circulations such as the Deacon cell (Döös and Webb, 1994). In an isopycnal averaging framework (Nurser and Lee, 2004a), the Deacon cell is reduced and therefore the isopycnal meridional transport streamfunction, i.e. the zonally integrated meridional transport of fluid across a given y and denser than a given density, is considered as a more appropriate description of the meridional overturning circulation (MOC). In order to obtain a physically meaningful MOC in the Eulerian framework, the initial simplification (i.e. the insensitivity of the transport integration to the physical state of the fluid) has to be revised and a more complicated redefinition of the total overturning streamfunction has to be introduced. More precisely, two different approaches of constructing physically more satisfying overturning streamfunctions in the Eulerian framework have been put forward: the residual-mean theory (Andrews and McIntyre, 1976; Eden et al., 2007) and the quasi-Stokes streamfunction (McDougall and McIntosh, 2001; Nurser and Lee, 2004b).

The residual streamfunction ψ_{res} is defined as the streamfunction which advects the Eulerian-mean buoyancy and it is constituted as the residual of two parts: On the one hand, the advection is due to the Eulerian-mean velocities (given by Λ), on the other hand, there is an eddy-induced streamfunction ψ^* due to the advective part of the eddy buoyancy flux. Physically, it is desired that, if there is no instantaneous diabatic buoyancy forcing, there should be also no diabatic effects in the Eulerian-mean buoyancy budget, i.e. the eddy-induced diabatic forcing should vanish too. Eden et al. (2007) (extending ideas of McDougall and McIntosh (1996); Medvedev and Greatbatch (2004)) demonstrate, by explicitly incorporating rotational eddy fluxes, that this physical criterion uniquely sets ψ^* and with it ψ_{res}. However, ψ^* is then given by a series involving fluxes of eddy buoyancy moments.

The quasi-Stokes streamfunction Ψ^* is the eddy-induced component of the total isopycnal streamfunction transformed into Eulerian space (McDougall and McIntosh, 2001; Nurser and Lee, 2004b). That is, the isopycnal streamfunction mapped into Eulerian space may be given by the sum of Λ and Ψ^* and advects the isopycnally averaged buoyancy[1]. McDougall and McIntosh (2001) (see also Nurser and Lee (2004b)) apply a Taylor

[1] The isopycnally averaged buoyancy is defined as inverse function of the mean height of isopycnals (de Szoeke and Bennett, 1993; McDougall and McIntosh, 2001; Nurser and Lee, 2004a).

series analysis centred around the mean height of isopycnals in order to express Ψ^* by Eulerian-mean quantities. Consequently, Ψ^* is given in two ways: On the one hand, it may be computed out of an isopycnal averaging framework. On the other hand, Ψ^* may be given directly in Eulerian space (i.e. in height coordinates) and is then expressed by a series expansion. Of course, this series expansion is different to the one of the residual-mean eddy streamfunction ψ^*, however, both are intimately connected as we discuss in this study.

Hence, if physically meaningful streamfunctions of the MOC are sought directly in the Eulerian framework, it seems that the appearance of series expansions generally represents a necessary and severe complication. Most problematic is that, practically, it is inevitable to cut off the series expansions at a certain order and hence one is left with approximate formulas. Typically, in a zonal-mean framework the first order terms of both series expansions are considered as good approximations in the nearly adiabatic ocean interior, but near horizontal boundaries (surface, bottom) the approximate formulas are found to break down, i.e. unphysical nonzero (and relatively large) values appear at the horizontal boundaries (Killworth, 2001; McDougall and McIntosh, 2001; Nurser and Lee, 2004b). A physically satisfactory solution of this serious problem is outstanding.

In this study, this problem will be further explored. The subjects of this study are the following: We formally compare for the first time (at least to our knowledge) the first three orders of the series expansions of ψ^* and Ψ^* in order to specify the essential differences between these two intimately linked streamfunctions at low orders. Furthermore, we consider all terms up to the third order of both series expansions in different idealised models of the Southern Ocean (SO) in order to investigate the behaviour of both series expansions in different concrete model setups which have been previously used to analyse eddy streamfunctions. It will turn out that, in a zonal-mean framework, the problems due to the convergence behaviour of both series expansions are more severe and hence the limitations of both approaches are stronger than discussed so far. Finally, we propose a measure to diagnose regions in the ocean where approximations of the series expansions break down.

The study is structured as follows: In section 2 we present our different model setups and experiments. In section 3 we consider approximations of the series expansion of the residual-mean eddy streamfunction ψ^*, while in section 4 we additionally examine approximations of the Taylor series of the quasi-Stokes streamfunction Ψ^*. Finally, in section 5 we propose the series number as a measure to diagnose the break down of the approximations and section 6 provides a summary and discussion.

2 Models and experiments

In this study, we use the code of CPFLAME[2] in two different configurations which both have been previously used to analyse eddy streamfunctions. The first configuration is essentially a reproduction of the model setup considered in the study of Nurser and Lee

[2] *http://www.ifm.zmaw.de/∼cpflame*

(2004a,b), who used an idealised eddy-permitting zonal channel model in order to compare the isopycnal transport streamfunction with the first order approximation of the quasi-Stokes streamfunction given by Eulerian-mean quantities. In our version, the primitive equations are formulated in Cartesian coordinates. The zonally reentrant channel extends over $L_x = 600$km in zonal direction and $L_y = 1000$km in meridional direction with 10km horizontal resolution. It is 1000m deep with 20m vertical resolution. The beta-plane approximation is used with a reference latitude situated at 49.31°S, such that at the centre of the channel the Coriolis parameter becomes the one at 45°S for spherical coordinates. We simulate only buoyancy b in the model, which might be thought as proportional to temperature. The model is not forced with winds, but the circulation in the model is driven by three buoyancy restoring regions: At the surface, b is relaxed towards a target buoyancy varying linearly between $21.764 \times 10^{-3}\text{ms}^{-2}$ at $y = 95$km and $45.269 \times 10^{-3}\text{ms}^{-2}$ at $y = 905$km with a restoring time scale of 7 days. Within the southernmost 95km and the northernmost 95km, model buoyancies are relaxed throughout the water column to specified values: linearly varying with depth from $19.346 \times 10^{-3}\text{ms}^{-2}$ at the surface to zero at the bottom in the southern zone and from $48.365 \times 10^{-3}\text{ms}^{-2}$ to zero in the northern zone. The relaxation rate varies linearly between 1/(2 days) at the boundaries, and zero at the inner edges of the relaxation zone. Vertical viscosity is $5 \times 10^{-4}\text{m}^2\text{s}^{-1}$ and we use a horizontal biharmonic viscosity of $1.25 \times 10^{11}\text{m}^4\text{s}^{-1}$. The linear bottom friction parameter is $2 \times 10^{-5}\text{s}^{-1}$. Vertical diffusivity is $5 \times 10^{-5}\text{m}^2\text{s}^{-1}$, but we use no explicit lateral diffusion. The Quicker advection scheme is used as the advection scheme of buoyancy. The model was run for a total of 30 years. The diagnostics below are presented as temporal averages over the last 10 years of the run. We refer to this experiment as the *NL case*.

The second configuration is the idealised SO model setup introduced and discussed by Viebahn and Eden (2010, 2012), i.e. an eddy-permitting primitive equation model consisting of a zonally reentrant channel, which is connected to a northern ocean basin enclosed by land. The circulation in the model is driven by a sinusoidal westerly wind stress over the channel with a magnitude of $\tau = 1 \times 10^{-4} m^2 s^{-2}$, and a surface restoring boundary condition for buoyancy b (again, there is only buoyancy in the model). The corresponding target buoyancy increases northward over the channel, remains constant over the southern half of the northern ocean basin and decreases while approaching the northern end of the domain. Boundary conditions on the northern and southern edges of the domain are simply given by no-flux conditions. Hence, the water mass distribution is solely determined by the surface boundary conditions. The domain of the idealised model extends over $L = 2520$km in the zonal and meridional direction, with 20km horizontal resolution and 40 vertical levels with 50m thickness (1900m maximal water depth). The channel (i.e. the SO) extends from the southern boundary ($x = 0$km) to $x = L/2$. Further details may be found in Viebahn and Eden (2010, 2012). In particular, we consider the same two experiments already discussed by Viebahn and Eden (2012) in an isopycnal averaging framework. In the *flat case* experiment, the bottom is completely flat. In the *hill case* experiment, a simple hill-like topographic feature is imposed in the channel: The top of the hill is located at $z = -950$m and $x = 0$ (and $x = 2520$km respectively). According to an exponential map the height of the hill decreases eastward (westward), such that at the

longitudes of the northern ocean basin (from $x = 850$km to $x = 1690$km) the channel has a flat bottom. In both experiments, the model has been run for 240 years. Additionally, we introduced harmonic viscosities (which act to damp EKE) in both experiments, in order to discuss the convergence behaviour of the series expansions of both ψ^* and Ψ^* subject to the "strength" of the eddy field. In the flat case, we introduced $A_h = 2000\text{m}^2\text{s}^{-1}$ and the model has been run for another 50 years, i.e. 290 years in total. In the hill case, we introduced $A_h = 2000\text{m}^2\text{s}^{-1}$, $A_h = 5000\text{m}^2\text{s}^{-1}$ and $A_h = 10000\text{m}^2\text{s}^{-1}$ respectively after 200 years of the initial model run and the model has been run for another 60 years, i.e. 260 years in total. In each experiment the time-mean is performed over the last 10 years[3].

In a way, the NL case represents the simplest model configuration in this study: Due to the lack of both zonal wind stress and the connection to a northern ocean basin, the time-zonal-mean meridional velocity $\overline{v}$ disappears almost completely in the NL case and hence it holds $\Lambda \approx 0$, in contrast to the wind-driven flat case and the hill case experiments. Since Λ generally opposes the eddy-induced streamfunctions in the SO, the wind-driven model configuration shows eddy-induced streamfunctions of higher magnitudes at equal magnitudes of the overall overturning circulation.

3 Approximations of the residual-mean streamfunctions

The time-zonal-mean residual streamfunction $\psi_{res}(y, z)$ is defined as the meridional streamfunction, which advects the Eulerian time-zonal-mean buoyancy $\overline{b}$. As outlined in appendix A, it is given by the sum of the time-zonal-mean Eulerian streamfunction Λ (defined by Eq. (14)) and the eddy streamfunction ψ^*,

$$\psi_{res} = \Lambda + \psi^* \ . \tag{1}$$

A physically consistent determination of ψ^* (and with it ψ_{res}) was given by Eden et al. (2007) by explicitly incorporating rotational eddy fluxes (see appendix A for a synopsis). ψ^* is then given by a series involving fluxes of eddy buoyancy moments (see Eq. (22)),

$$\psi^* |\nabla \overline{b}| = -J_1 + \partial_m J_2 - \frac{1}{2}\partial_m^2 J_3 + O(b'^4) \ , \tag{2}$$

where $\partial_m() \equiv |\nabla\overline{b}|^{-1}\nabla\overline{b} \cdot \nabla|\nabla\overline{b}|^{-1}()$ and the $J_n \equiv \mathbf{F}_n \cdot \underset{\neg}{\nabla}\overline{b}|\nabla\overline{b}|^{-1}$ represent the along-isopycnal fluxes of the eddy buoyancy moments[4]. The terminology $O(b'^4)$ indicates ad-

[3] Note that in this study, we perform the analysis in a time-zonal-mean context. That is, each quantity q generally may be decomposed into its temporal and zonal average $\overline{q}$ and its temporal and zonal deviation $q' \equiv q - \overline{q}$, i.e. $q = \overline{q} + q'$. However, we denote the time-zonal-mean by an overbar only regarding the basic physical quantities, i.e. the velocities and buoyancy. The meridional streamfunctions considered in this study are zonally integrated quantities from the outset and we do not explicitly denote the additional time average by another symbol, but implicitly assume it from now on.

[4] The eddy buoyancy moments are defined as $\phi_n = b'^n/n$ and the fluxes of the eddy buoyancy moments are given by $\mathbf{F}_n = L_x(\overline{v\phi_n}, \overline{w\phi_n})$, where n represents the order. The operator $\underset{\neg}{\nabla}$ is defined as $\underset{\neg}{\nabla} \equiv (-\partial_z, \partial_y)$. See appendix A for more details.

ditional terms that are of fourth or higher order in buoyancy perturbations. The orders of the series expansion (2) are defined solely by the fluxes of b'^n, i.e. via the order of the eddy buoyancy moment. The first order term in the expansion for ψ^* is identical to an eddy streamfunction of the transformed Eulerian mean (TEM) framework (Andrews and McIntyre, 1976, 1978b). The remainder of the expansion is due to the introduction of the rotational flux potential θ (see Eq. (23)). In the interior ocean, it typically holds $|\partial_y \bar{b}| \ll |\partial_z \bar{b}|$ and $|w| \ll |v|$ and we obtain

$$\psi^* \approx \frac{L_x \overline{v'b'}}{\partial_z \bar{b}} - \frac{1}{\partial_z \bar{b}} \partial_z \left(\frac{L_x \overline{\phi_2 v}}{\partial_z \bar{b}} \right) + \frac{1}{2} \frac{1}{\partial_z \bar{b}} \partial_z \left(\frac{1}{\partial_z \bar{b}} \partial_z \left(\frac{L_x \overline{\phi_3 v}}{\partial_z \bar{b}} \right) \right) + O(b'^4) \tag{3}$$

Now we consider the first three orders of the series expansion of the residual-mean eddy streamfunction ψ^* in our different model experiments. Notice that we calculated the terms as given by Eq. (2), but that differences to the terms as given by Eq. (3) are small in the entire model domain (including the diabatic boundary regions). In the following, we index the terms of the different orders of the series expansion of ψ^* by Roman numerals, i.e. $\psi^* = \psi^*_I + \psi^*_{II} + \psi^*_{III} + \psi^*_{IV} + ...$

3.1 NL case

Fig. 1 a) shows the first term $\psi^*_I \equiv -J_1/|\nabla \bar{b}|$ of the series expansion of ψ^* (see Eq. (2)), i.e. the TEM eddy streamfunction, and Fig. 1 d) shows $\Lambda + \psi^*_I$, i.e. the TEM residual MOC of the NL case. Since $\Lambda \approx 0$ (not shown) due to the lack of zonal wind stress, both are largely identical, showing an anti-clockwise MOC with mainly along-isopycnal flow in the ocean interior and strong diapycnal flow in the three buoyancy restoring regions (but no bottom boundary layer). Only at mid-depth around $y = 750$km, the TEM residual MOC is slightly reduced in magnitude compared to ψ^*_I. However, physically inadequate is the extremely strong recirculation cell in the surface layer, which does not tend to zero at the surface (in Fig. 1 we simply set the surface values to zero).

Nurser and Lee (2004b) find a similar circulation pattern (see their Fig. 1). They discuss the unphysical surface circulation in the context of the classical TEM formalism, but the approaches of solving the problems at the boundaries by merging different eddy streamfunctions into each other are only partially successful and of unclear physical basis, hence remain unsatisfactory. In the physically logical approach of Eden et al. (2007), which we adopt in this study (see appendix A for a synopsis), the problems at the boundaries are theoretically solved by incorporating the appropriate rotational eddy flux (given by Eq. (23)). However, since the appropriate rotational eddy flux is only given by a series expansion, the practical problem of including a sufficient number of terms of the series expansion in order to obtain an adequate approximation emerges.

Fig. 1 b,c) show the second term ψ^*_{II} and the third term ψ^*_{III} of the series expansion of ψ^*. In line with the expectation that ψ^*_I represents a good approximation of ψ^* in the nearly adiabatic ocean interior, the dominant values of the next higher order terms ψ^*_{II} and ψ^*_{III} are found in the surface diabatic boundary layer (for ψ^*_{IV} and ψ^*_V as well, not shown),

although changes of the corresponding residual MOCs (Fig. 1 e,f)) are also visible in the ocean interior (compare also Fig. 1 d-f) with Fig. 5 a)). More precisely, ψ^*_{II} mainly opposes the surface layer circulation of ψ^*_I, while ψ^*_{III} amplifies it again. Hence, the series expansion (2) (or Eq. (23)) appears to be alternating, which is obvious in Fig. 1 a-c) and continued for the next higher order terms ψ^*_{IV} and ψ^*_V (not shown). This behaviour hampers the determination of an order at which the series expansion may be appropriately cut off, since the next higher order always compensates a part of the previous order. Moreover, it holds $|\psi^*_{II}| < |\psi^*_{III}|$ in the surface layer. More generally, the ratio $|\psi^*_i|/|\psi^*_I|$ (not shown) increases with increasing order i in the surface boundary layer, while it decreases in the ocean interior. That is, the magnitude of the terms of the series expansion (23) appears to be increasing in the diabatic surface region with increasing order, while a decreasing behaviour, which is found in the ocean interior, is necessary for an adequate approximation of ψ^* by low order terms.

We conclude: In the NL case, the series expansion of ψ^* may be adequately approximated by low order terms in the ocean interior, since there they appear to be decreasing with higher order - ψ^*_I alone already may seem sufficient (but notice section **??**). However, in the diabatic surface boundary layer the series expansion of ψ^* is alternating and initially increasing[5], which precludes an adequate approximate surface layer representation by low order terms, i.e. leads to the "break down" of an approximation of ψ^*. Hence, the series approach of Eden et al. (2007) seems to be unable to practically solve the problems at the boundaries appearing in the residual-mean framework.

3.2 Flat case

Fig. 2 a) shows ψ^*_I, i.e. the TEM eddy streamfunction of the flat case, which shows the well-known eddy-induced streamfunction behaviour in the SO (extending from $x = 0$km to $x = L/2$): A strong negative circulation pattern, which opposes the positive circulation pattern of Λ (not shown, see e.g. Viebahn and Eden (2012)) in the SO, such that the sum of both, i.e. the TEM residual streamfunction shown in Fig. 2 d), is given by two global overturning cells. Namely, a positive circulation cell which connects the SO and the Atlantic and a bottom reaching negative circulation cell. We notice that, on the one hand, the residual MOC in the SO is of equal magnitude as the residual MOC of the NL case[6], but, on the other hand, the magnitude of ψ^*_I is significantly larger, since Λ is not small. However, we find problems at the boundaries analog to the problems already encountered in the NL case. ψ^*_I now shows large and unphysical[7] negative recirculation cells in the surface

[5] In this study, we call a series expansion $s = \sum_{i=1}^{\infty} s_i$ *increasing* (or *decreasing*), if the magnitude of the terms of s is increasing (or decreasing) with higher order i, i.e. $|s_i| < |s_{i+1}|$ (or $|s_i| > |s_{i+1}|$).

[6] That is, the water mass transformations are similar in both cases (Walin, 1982; Marshall and Radko, 2003).

[7] We note that "unphysical" primarily means that ψ^*_I does not tend to zero at the horizontal boundaries, while, for averaging along latitude circles, negative recirculation cells at the surface are also found in an isopycnal averaging framework - as shown for both the flat case and the hill case in Fig. 5 b,c) and discussed by Viebahn and Eden (2012).

boundary layer and in the bottom boundary layer in the SO, which are also present in the TEM residual MOC $\Lambda + \psi_I^*$. Due to the coarser vertical resolution of our second model configuration, we can not discuss in detail the boundary layer behaviour of the next higher order terms of the series expansion of ψ^*. Nevertheless, the few boundary layer values suggest the same unsolved practical problem as in the NL case, namely, next higher order terms ψ_i^* of increasing magnitude such that an adequate approximate boundary layer circulation given by low order terms is impossible.

But we can consider the behaviour of the subsequent terms of the series expansion of ψ^* in the ocean interior. Fig. 2 b,c) show ψ_{II}^* and ψ_{III}^*. As expected, ψ_I^* dominates over ψ_{II}^* and ψ_{III}^* in the interior of the SO. However, both ψ_{II}^* and ψ_{III}^*, although being smaller than ψ_I^* everywhere in the interior of the SO, show magnitudes of the same order as ψ_I^* below $z = -950$m and at mid-depth around $y = 1000$km. Moreover, we notice the strong changes in the diabatic northern convective region. Hence, both terms induce significant changes in the residual MOC (Fig. 2 e,f)): Especially, the negative circulation cell changes both magnitude and circulation pattern by the inclusion of each term. In case both ψ_{II}^* and ψ_{III}^* are included (Fig. 2 f)), the streamlines of the residual MOC in the SO are significantly more aligned along the time-zonal-mean isopycnals in the interior (compare Fig. 2 d-f) with Fig. 5 b,e)). Hence, in the flat case the inclusion of the next higher order terms ψ_{II}^* and ψ_{III}^* distinctly improves the approximation of ψ^* by ψ_I^* alone.

Furthermore, ψ_{II}^* mainly opposes the interior circulation of ψ_I^*, while ψ_{III}^* largely amplifies it. That is, the series expansion of ψ^* is again alternating (similar to the NL case), which is obvious in Fig. 2 a-c) and continued for the next higher order terms ψ_{IV}^* and ψ_V^* (not shown). However, with increasing order i the ratio $|\psi_i^*|/|\psi_I^*|$ (not shown) decreases in the interior of the SO, which suggests that the desired behaviour of an in general decreasing series expansion essentially holds in the interior of the SO. We can conclude: In the flat case, the series expansion of ψ^* is alternating and may be adequately approximated by low order terms in the ocean interior, since there they appear to be decreasing. However, the next higher order terms ψ_{II}^* and ψ_{III}^* significantly improve an approximation of ψ^* by ψ_I^* alone. Hence, the series approach of Eden et al. (2007) represents an advancement of the description of the ocean interior circulation within the residual-mean framework.

Now, in order to minimise the impact of the next higher order terms ψ_{II}^* and ψ_{III}^*, i.e. in order to obtain a faster convergence of the series expansion of ψ^* in the interior of the SO, we introduced a harmonic viscosity of $A_h = 2000\text{m}^2\text{s}^{-1}$ in the flat case. A_h acts to damp EKE and hence the corresponding TEM eddy streamfunction ψ_I^*, shown in Fig. 2 g), has a weaker but still strong negative circulation cell in the SO (while the negative circulation in the northern convective region is increased and extended). The TEM residual MOC, i.e. $\Lambda + \psi_I^*$ (Fig. 2 j)), shows a significantly weaker bottom reaching negative circulation cell, while the global positive circulation cell extends much deeper, but remains of the same magnitude in the SO (of course, also Λ (not shown) changes). The next higher order terms ψ_{II}^* and ψ_{III}^* shown in Fig. 2 h,i) (as well as ψ_{IV}^* and ψ_V^*, not shown) are now significantly reduced (except for an increase in the northern convective region), such that in the interior of the SO, ψ^* is essentially given by ψ_I^*. Only in a small band at mid-depth around $y = 1000$km the next higher order terms ψ_{II}^* and ψ_{III}^* show significant values,

which almost disappear for ψ^*_{IV} and ψ^*_V (not shown). The reduced impact of the next higher order terms is more accurately expressed by the behaviour of the ratio $|\psi^*_i|/|\psi^*_I|$ (not shown), which is also drastically reduced in the interior of the SO. Consequently, in the flat case the impact on the TEM eddy streamfunction ψ^*_I by the gauge potential introduced by Eden et al. (2007) (see Eq. (23)) related to rotational eddy fluxes depends directly on the "strength" of the eddy field, i.e. the magnitude of the EKE. Hence, if the EKE is adequately reduced, it seems acceptable to approximate ψ^* by ψ^*_I in the nearly adiabatic interior of the SO in the flat case. We notice that the series expansion remains alternating and note that in the diabatic regions at the surface, at the bottom and at the northern and southern boundaries convergence is far from being reached by including the first three orders (see Fig. 2 g-i)).

3.3 Hill case

Fig. 3 a) shows the TEM eddy streamfunction ψ^*_I of the hill case. Compared to the flat case, the negative circulation is reduced at topographic depths, in particular a bottom boundary layer is absent. This is in accordance with the geostrophic return flow of Λ (not shown, see Viebahn and Eden (2012)) in the hill case, which extends over the depth range below the hill depth and is not confined to a bottom boundary layer as in the flat case. On the other hand, the number of local maxima in ψ^*_I is increased: One local maximum is found above topography around $y = 800$km and 500m depth. Moreover, meridional recirculation cells appear around the hill depth[8] ($z = -950$m), which induce a negative and a positive recirculation cell around the hill depth in the TEM residual MOC $\Lambda + \psi^*_I$ (Fig. 3 d)). These recirculation cells represent strong diapycnal flow and hence contradict the physical picture of a nearly adiabatic flow in the interior of the SO. Consequently, we would expect the next higher order terms to reduce these cells in order to obtain a physically more consistent circulation pattern.

Fig. 3 b,c) show ψ^*_{II} and ψ^*_{III}. While ψ^*_{II} and ψ^*_{III} exhibit the same circulation pattern in the Atlantic part as in the flat case, they are drastically increased in the SO part, in particular around the hill depth (along the entire meridional extension of the SO) and above topography (around $y = 800$km and 400m depth). The maximal values now lie around the hill depth and not near the bottom as in the flat case. ψ^*_{II} partially compensates for the spurious diabatic recirculation cells in the residual MOC $\Lambda + \psi^*_I$ with a negative circulation around $y = 900$km and a positive circulation around $y = 400$km at the hill depth. Nevertheless, the inclusion of ψ^*_{II} appears to overcompensate (Fig. 3 e)): The number and the magnitude of the recirculation cells around the hill depth and above topography is increased such that the overall circulation pattern becomes more unphysical. This tendency of intensifying the recirculation cells and complicating the circulation pattern continues, if ψ^*_{III} is included (Fig. 3 f)).

Furthermore, the magnitude of ψ^*_{III} is even larger than the magnitude of ψ^*_{II} for most

[8] Note that in the isopycnal eddy streamfunction meridional recirculation cells around the hill depth do not appear, as shown by Viebahn and Eden (2012). See also Fig. 5 c).

parts of the SO. More precisely, we find that with increasing order i the ratio $|\psi_i^*|/|\psi_I^*|$ (not shown) increases in the interior of the SO, with values greater 1 around the hill depth already for $i = II$. As in the flat case, the next higher order terms ψ_{II}^* and ψ_{III}^* (also ψ_{IV}^* and ψ_V^*, not shown) of the series expansion of ψ^* still show a type of alternating behaviour, but the behaviour of a decreasing series expansion seems to be completely lost in the hill case.

This drawback of a, at least initially, increasing series expansion does not disappear, if a harmonic viscosity A_h is introduced in the hill case[9]. By increasing A_h, expectedly the overall magnitude of the TEM eddy streamfunction ψ_I^* decreases. Moreover, the circulation pattern of ψ_I^* deforms with increasing A_h, such that the negative recirculation cell at the hill depth of the residual MOC $\Lambda + \psi_I^*$ decreases. For example, if $A_h = 10000\mathrm{m}^2\mathrm{s}^{-1}$ is used, the negative circulation cell of the TEM residual MOC is nearly void of recirculation cells in the nearly adiabatic interior, but the accompanying positive recirculation cell is drastically increased. While $A_h = 2000\mathrm{m}^2\mathrm{s}^{-1}$ has a rather small impact on ψ^* and the residual MOC in the hill case, $A_h = 5000\mathrm{m}^2\mathrm{s}^{-1}$ leads to the strongest reduction of the next higher order terms ψ_{II}^* and ψ_{III}^* (in particular above topography) for our set of A_h values. Nevertheless, for all three values of A_h the next higher order terms ψ_i^* (we considered terms up to $i = V$) conserve the previous features: In an alternating manner, the magnitudes increase and the circulation patterns complicate with higher orders i. In particular, the ratios $|\psi_i^*|/|\psi_I^*|$ (not shown) increase in the SO with more and more regions in the SO of values greater than 1.

Consequently, in the hill case the series expansion of ψ^* may not have a reasonable cut off, since it seems to be, at least initially, an increasing series expansion in broad regions of the SO. Now even in the interior the residual-mean approach, both in its classical TEM version and in its advancement by Eden et al. (2007), is dissatisfying.

4 Comparison with the quasi-Stokes streamfunction

Assuming that the buoyancy field $b(x, y, z, t)$ is vertically strictly monotonic in the entire ocean, the instantaneous isopycnal b_a lies at an instantaneous height $z(x, y, b_a, t) = z_a(y, b_a) + z_a'(x, y, b_a, t)$, where z_a is the time-zonal-mean height of b_a and z_a' is the deviation from the time-zonal-mean, i.e. $\overline{z_a'} = 0$. The time-zonal-mean isopycnal streamfunction ψ_I is then the temporally averaged and zonally integrated meridional transport below the instantaneous isopycnal b_a. We may write

$$\psi_I(y, b_a) = -L_x \overline{\int_{bottom}^{z_a + z_a'} v \; dz} \; . \tag{4}$$

ψ_I may be transformed to Eulerian space by identifying each b_a with its mean height z_a. Therewith, the quasi-Stokes streamfunction Ψ^* is defined via the decomposition

$$-L_x \overline{\int_{bottom}^{z_a + z_a'} v \; dz} = \Lambda(y, z_a) + \Psi^*(y, z_a) \; , \tag{5}$$

[9] We do not show further hill case figures due to their physical disqualification.

that is,

$$\Psi^*(y, z_a) \equiv -L_x \overline{\int_{z_a}^{z_a+z'_a} v \; dz} \; , \tag{6}$$

and gives the transport of ψ_I related to the perturbation z'_a. Ψ^* is the eddy-induced streamfunction of ψ_I in Eulerian space[10]. Expressions of both z'_a and Ψ^* by Eulerian mean quantities may be obtained by expanding b and v in Taylor series centred around z_a (McDougall and McIntosh, 2001; Nurser and Lee, 2004b) as outlined in appendix B. If we define the orders of the series expansion by the perturbations of b in order to obtain a form comparable to the residual-mean framework (see Eq. (2) and Eq. (3)), we find the following series expansion for Ψ^* expressed by Eulerian mean quantities (extending the approximations of previous studies, see appendix B)

$$\Psi^* \;\; = \;\; \Psi^*_I + \Psi^*_{II} + \Psi^*_{III} + O(b'^4) \; , \tag{7}$$

where

$$\Psi^*_I \;\; = \;\; \frac{L_x \overline{b'v'}}{\partial_z \overline{b}} = \psi^*_I \tag{8}$$

$$\Psi^*_{II} \;\; = \;\; -\frac{1}{\partial_z \overline{b}} \partial_z \Big(\frac{L_x \overline{\phi_2 v}}{\partial_z \overline{b}} \Big) + \frac{\overline{v}}{\partial_z \overline{b}} \partial_z \Big(\frac{L_x \overline{\phi_2}}{\partial_z \overline{b}} \Big) = \psi^*_{II} + \psi^*_{\Delta II} \tag{9}$$

$$\begin{aligned} \Psi^*_{III} \;\; = \;\; & \frac{1}{2} \frac{1}{\partial_z \overline{b}} \partial_z \Big(\frac{1}{\partial_z \overline{b}} \partial_z \Big(\frac{L_x \overline{\phi_3 v}}{\partial_z \overline{b}} \Big) \Big) - \\ & -\frac{1}{2} \frac{\overline{v}}{\partial_z \overline{b}} \partial_z \Big(\frac{1}{\partial_z \overline{b}} \partial_z \Big(\frac{L_x \overline{\phi_3}}{\partial_z \overline{b}} \Big) \Big) - \frac{L_x^{-1}}{\partial_z \overline{b}} \partial_z \Big(\frac{L_x \overline{\phi_2}}{\partial_z \overline{b}} \Big) \partial_z \Big(\frac{L_x \overline{v'b'}}{\partial_z \overline{b}} \Big) \\ = \;\; & \psi^*_{III} + \psi^*_{\Delta IIIa} + \psi^*_{\Delta IIIb} \end{aligned} \tag{10}$$

4.1 Formal comparison of ψ^* and Ψ^*

It is obvious that the complete series expansions of ψ^* and Ψ^* are essentially different, since ψ^* and Ψ^* advect different time-zonal-mean buoyancy distributions. However, the corresponding time-zonal-mean buoyancy distributions mainly differ in the boundary layers, while in the nearly adiabatic interior of the ocean they are generally found to be similar (Killworth, 2001; Nurser and Lee, 2004a; Viebahn and Eden, 2012). Hence, the two streamfunctions are expected to be similar there too.

By comparing Eq. (7) with Eq. (3), the similarity of ψ^* and Ψ^* is suggested by the identity of the first order terms. However, we find that with increasing order the series expansions of ψ^* and Ψ^* deviate more and more from each other. The difference between the second order terms, $\psi^*_{\Delta II}$, is given by a term including the time-zonal-mean meridional velocity, which is generally small in a zonal channel. The difference between the third order terms is constituted by a corresponding term, $\psi^*_{\Delta IIIa}$, including the time-zonal-mean

[10] In Viebahn and Eden (2012) the corresponding decomposition is defined in an isopycnal framework.

meridional velocity and an additional term, $\psi^*_{\Delta III b}$, of a type not present in the residual-mean series expansion, namely, a product of a first order term (the vertical derivative of Ψ^*_I) with a second order term (a variance term). For higher order terms we expect even more complicated discrepancies, especially further products between different orders, i.e. types of terms not present in the residual-mean series expansion.

Moreover, only in case of Ψ^* we are able to compute the streamfunction directly in an isopycnal framework without referring to the series expansion (Nurser and Lee, 2004a; Viebahn and Eden, 2012). Hence, we know the result to which the series expansion of Ψ^* must converge. In case of ψ^*, we do not have another computational option besides the series expansion. Especially in the diabatic regions, the residual-mean circulation may therefore not be properly determined so far, as demonstrated in section 3. Furthermore, it is not even secure so far that the residual-mean series is a converging series expansion. Up to now, the advantage of the residual-mean series over series expansion of Ψ^* is that it is given in a compact and complete form, while we have not found a corresponding expression for the series expansion of Ψ^* yet.

Now we return to our three model experiments. In each case, we discuss the three additional terms appearing in Eq. (7) and not in Eq. (3), and we consider the streamfunctions to which the series expansion Ψ^* has to converge.

4.2 Differences between the approximations of ψ^* and Ψ^* in model experiments

In the NL case, both $\psi^*_{\Delta II}$ and $\psi^*_{\Delta III a}$ (not shown), related to $\overline{v} \approx 0$, essentially vanish, even in the surface boundary layer (as far as it is resolved). In contrast, the third order difference term $\psi^*_{\Delta III b}$ (not shown), related to the product of a variance term and an eddy buoyancy flux term, exhibits significant values in the surface boundary layer. Consequently, the difference between the terms of the series expansions of Ψ^* and ψ^* appears to increase with higher order. In accordance with our expectation, the differences $\psi^*_{\Delta II}$, $\psi^*_{\Delta III a}$ and $\psi^*_{\Delta III b}$ suggest that ψ^* and Ψ^* mainly differ in the diabatic surface layer, while they are similar in the nearly adiabatic ocean interior. More precisely, $\psi^*_{\Delta III b}$ is small and of the same sign as ψ^*_{III} (Fig. 1 c)) in the northern part of the channel, while $\psi^*_{\Delta III b}$ is significantly opposing ψ^*_{III} in the southern part of the channel. Hence, the maximal absolute values of Ψ^*_{III} are slightly smaller than those of ψ^*_{III}. This might indicate that the series expansion of Ψ^* converges faster then that of ψ^*. Nevertheless, the overall characteristics of the low order terms of the series expansion of Ψ^* remain those described in section 3.1.

In the flat case, the terms $\psi^*_{\Delta II}$, $\psi^*_{\Delta III a}$ and $\psi^*_{\Delta III b}$ (not shown) are small in the interior of the ocean, such that also the second and third orders of the series expansions of ψ^* and Ψ^* coincide in the ocean interior for the flat case (with characteristics described in section 3.2). In particular, the terms $\psi^*_{\Delta II}$ and $\psi^*_{\Delta III a}$ are small in the interior, although it holds $\overline{v} \neq 0$. Significant values of $\psi^*_{\Delta II}$, $\psi^*_{\Delta III a}$ and $\psi^*_{\Delta III b}$ are present in the northern convective region, while in the surface and bottom boundary layers they are only obvious for $\psi^*_{\Delta III b}$ (and probably lost due to the few vertical grid points and the smaller extension for $\psi^*_{\Delta II}$

and $\psi^*_{\Delta IIIa}$). The significant values tend to counteract the corresponding next higher order contributions shown in Fig. 2 b,c). Furthermore and similar to the NL case, the term of highest order in perturbation quantities, $\psi^*_{\Delta IIIb}$, exhibits the highest values in the northern convective region and in the southern bottom and surface boundary layers. This tendency of increasing compensation again might indicate that the series expansion of Ψ^* converges faster than the one of ψ^* in the diabatic regions in the flat case.

By including a harmonic viscosity of $A_h = 2000\mathrm{m}^2\mathrm{s}^{-1}$ in the flat case configuration (not shown), the situation is essentially unchanged: The terms $\psi^*_{\Delta II}$, $\psi^*_{\Delta IIIa}$ and $\psi^*_{\Delta IIIb}$ remain small in the ocean interior. In accordance with Fig. 2 h,i), the magnitudes of the significant values in the boundary regions are increased compared to the case of vanishing A_h, such that significant values also appear in $\psi^*_{\Delta II}$ in the surface layer. The term $\psi^*_{\Delta IIIb}$ still shows the highest values, in particular in the southern bottom and surface boundary layers of the SO, so that a tendency of increasing compensation is furthermore present.

So far all considered cases are in line with expectations: In the ocean interior ψ^* and Ψ^* essentially coincide, while in the boundary regions significant differences between ψ^* and Ψ^* are given by $\psi^*_{\Delta II}$, $\psi^*_{\Delta IIIa}$ and $\psi^*_{\Delta IIIb}$, such that the next higher order terms of the series expansion of Ψ^* tend to be smaller than the corresponding terms of ψ^*.

Turning to the hill case, the question is: Do the additional terms $\psi^*_{\Delta II}$, $\psi^*_{\Delta IIIa}$ and $\psi^*_{\Delta IIIb}$ add to the residual-mean terms at each order such that the series expansion of Ψ^* is decreasing and that the recirculation cells in the ocean interior, encountered in section 3.3, disappear? This is not the case. Fig. 4 a-c) show $\psi^*_{\Delta II}$, $\psi^*_{\Delta IIIa}$ and $\psi^*_{\Delta IIIb}$ for the hill case. In the basin part ($x > 1250$km), each term shows nearly the same pattern as in the flat case, similar to the terms ψ^*_I, ψ^*_{II} and ψ^*_{III} encountered in section 3.3. However, in the SO now significant values appear in the ocean interior. The second order term $\psi^*_{\Delta II}$, related to $\overline{v}$, exhibits a small negative recirculation cell around $y = 800$km at 1100m depth. This leads to a small reduction of the corresponding positive recirculation cell in Fig. 3 e), but the overall pattern remains unchanged (not shown). The same holds for the third order: Although $\psi^*_{\Delta IIIa}$, related to $\overline{v}$, vanishes, $\psi^*_{\Delta IIIb}$ induces a strong positive recirculation cell at the hill depth and a smaller one at mid-depth ($y = 900$km and $z = -400$m), which, however, only slightly change the circulation pattern of Fig. 3 f) (not shown). Consequently, also in the hill case we find that the significant values of the next higher order terms of the series expansion of Ψ^* tend to be reduced compared to than those of ψ^*. But the overall circulation pattern in not essentially changed by including the lower orders, so that the unphysical recirculation cells in the ocean interior remain.

Including a harmonic viscosity A_h in the hill case configuration does not change the situation. In case of $A_h \equiv 5000\mathrm{m}^2\mathrm{s}^{-1}$ (not shown), the magnitudes of both $\psi^*_{\Delta II}$ and $\psi^*_{\Delta IIIb}$ are reduced in the ocean interior, but still significant, while $\psi^*_{\Delta IIIa}$ now shows a negative recirculation cell around $y = 800$km at 1100m depth. However, the unphysical circulation patterns are only slightly changed by the inclusion of the quasi-Stokes terms (not shown). The analog situation is met if A_h is set to $A_h \equiv 10000\mathrm{m}^2\mathrm{s}^{-1}$ (not shown). Each term exhibits recirculation cells around the top of topography with drastically increased magnitudes. However, since the magnitudes of ψ_{II} and ψ_{III} are even more increased, the overall effect remains small (not shown).

For completeness we show in Fig. 5 the isopycnal streamfunction of the NL case (a), flat case (b) and hill case (c), and the corresponding mean isopycnals, which largely have been discussed in Nurser and Lee (2004a) and Viebahn and Eden (2012). Comparing Fig. 5 a) with Fig. 1 d-f) we again find that the interior circulation is significantly improved by the incorporation of the second and third order terms, while in the upper 200m convergence is far from being reached. In the flat case, comparing Fig. 5 b) and Fig. 2 d-f), the problems are slightly more severe, since also, beside the surface layer, in the northern convective region, the southern boundary and the bottom boundary layer in the SO convergence is far from being reached. Finally, the worst scenario we find in the hill case (compare Fig. 5 c) with Fig. 3 d-f)), where even the interior circulation of the SO becomes completely unphysical by including next higher order terms.

5 Series number

In sections 3 and 4, we demonstrated that an approximation of ψ^* and Ψ^* by low order terms of their series expansion is impossible in certain regions of the ocean, since the series expansion of ψ^* and Ψ^* are increasing there. These regions are mainly the horizontal boundary layers, which are generally characterised by diabatic processes, i.e. by large diapycnal diffusivities. A serious aggravation we found in the more realistic hill case, where the series expansion of ψ^* and Ψ^* are also initially increasing at mid-depth above topography. We are able to give an indicator of whether the series expansion of ψ^* is initially increasing or decreasing by consulting the results of Eden et al. (2009). Since the increasing behaviour of the series expansion of Ψ^* is similar to the one of ψ^* in our model experiments, S may also apply to Ψ^*.

Eden et al. (2009) were able to derive the generalised Osborn-Cox relation,

$$\kappa + \mu = \mu \overline{(1 + C) \exp(-Db')} \ , \tag{11}$$

which relates the turbulent diapycnal diffusivity κ to the molecular diffusivity μ, the Cox number $C = |\nabla b'|^2/|\nabla \bar{b}|^2$ and the dimensionless ratio Db' relating the buoyancy perturbation with the mean curvature scale $D = (\nabla^2 \bar{b})/|\nabla \bar{b}|^2$. The ratio Db' appears in the argument of the exponential map, which represents a standard example of a converging series which is initially increasing, if the argument is greater than 1. Hence, as a measure of whether the series expansion of κ, given by Eq. (11), is initially increasing or decreasing, we define the *series number*,

$$S \equiv |D| \sqrt{2\overline{\phi_2}} \ , \tag{12}$$

such that we expect for $S > 1$ (or near 1) an initially increasing series expansion. Since κ appears on the one side and ψ^* on the other side of the Eulerian mean buoyancy budget (see Eq. (16) in appendix A), we carry this criterion over to the series expansion of ψ^*.

Fig. 6 a) shows S for the NL case. As expected, we find $S > 1$ only in the surface boundary layer. Below the surface boundary layer, it holds $S < 1$, with the highest values

near the bottom. Fig. 6 b) shows S for the flat case. We find $S > 1$ in the southern surface boundary layer, the northern convective region and in the bottom boundary layer[11]. In the ocean interior of the SO, it holds $S < 1$. Introducing A_h (not shown) generally decreases S in the interior of the SO, but increases S in the boundary layers and in the Atlantic part. Finally, Fig. 6 c) shows S for the hill case. As expected, we find $S > 1$ now at the top of topography and not at the bottom in the SO, while in the rest of the ocean interior it holds $S < 1$. In particular, at mid-depth above topography in the SO, where the series expansion of ψ^* is initially increasing, S is increased compared to the flat case, but we still have $S < 1$. Hence, in regions of smaller diapycnal diffusivity the criterion is of reduced evidence. For $A_h = 5000\mathrm{m}^2\mathrm{s}^{-1}$ the series number S decreases at the hill depth, but it still holds $S > 1$ (not shown). For $A_h = 10000\mathrm{m}^2\mathrm{s}^{-1}$ the series number S is again drastically increased in the entire domain (not shown).

Consequently, in the diabatic boundary regions and at topographic depths the series number S represents a successful[12] measure in our model experiments of whether the series expansion of ψ^* is, at least initially, increasing or not, while in the nearly adiabatic interior above topography the criterion is of reduced evidence in the hill case.

6 Summary and discussion

In this study, we have considered the series expansion of the residual-mean eddy streamfunction ψ^* and the Taylor expansion of the quasi-Stokes streamfunction Ψ^* up to third order in buoyancy perturbation b'. Beside a formal comparison, we analysed the resulting MOCs at each order in three different eddy-permitting numerical model experiments which have been previously used to analyse eddy streamfunctions, namely the NL case experiment, which is essentially a reproduction of the idealised zonal channel model setup considered by Nurser and Lee (2004a,b), and the flat case and hill case experiments of the idealised SO model setup introduced by Viebahn and Eden (2010, 2012).

Formally, the series expansions of ψ^* and Ψ^* increasingly differ from each other with increasing order. While the first order terms are identical, the difference between the second order terms is related to the time-zonal-mean meridional velocity $\overline{v}$. Since $\overline{v}$ is generally small in a zonal channel, the second order difference may be expected to be small there as well. The third order difference is constituted by a corresponding term related to $\overline{v}$ and an additional term, which is related to v' and, hence, is of fourth order in perturbation quantities b' and v'. For orders higher than three, we expect the emergence of further types of terms related to v'. Regarding a zonal channel, it is likely that the terms related to v' primarily need to be considered in order to distinguish between ψ^* and Ψ^*.

This expectation is confirmed in each of our three model experiments, where the third

[11] In the boundary layer of the SO, the values of S are around 0.96 (and the lowest two grid points are missing due to the second order derivatives), while in the cases with A_h, S significantly exceeds 1 in the bottom boundary layer of the SO.

[12] Notice that the ratios $|\psi_i^*|/|\psi_I^*|$ (not shown) generally are greater than 1 in the bottom boundary layer of the Atlantic part, so that $S > 1$ is appropriate there.

order difference term related to v' shows the largest magnitudes. Hence, at least initially and in regions of significant values, the magnitudes of the differences between ψ^* and Ψ^* tend to increase with higher order. Significant differences between the terms of the series expansion of ψ^* and the Taylor series of Ψ^* are present in the diabatic boundary regions in the NL case and the flat case, while in the hill case differences are also found in the ocean interior (around hill depth and above[13]). In the NL case and the flat case, this is in accordance with the expectation that both streamfunctions largely coincide in the nearly adiabatic interior, since the corresponding mean buoyancy distributions largely coincide there (Nurser and Lee, 2004a; Viebahn and Eden, 2012). Finally, we find that the terms of Ψ^* generally tend to have smaller magnitudes than the corresponding terms of ψ^*, which might indicate that the series expansion of Ψ^* converges faster than that of ψ^*.

However, despite significant differences in certain regions, the series expansion of ψ^* and the Taylor series of Ψ^*, considered up to the third order in our model experiments, show the same behaviour in several aspects: Both series expansions generally tend to be of alternating character, such that the next higher order always compensates a part of the previous order. Furthermore, in the NL case and the flat case, both series expansions may be adequately approximated by low order terms in the ocean interior, since there they appear to be decreasing with higher order. Nevertheless, including terms up to the third order still significantly improves the interior circulations in these two cases, in the sense that they further approach the corresponding circulation patterns of the isopycnal streamfunction and that streamlines become more aligned along the mean isopycnals in the ocean interior. For the flat case, we showed that the impact of the next higher order terms in the ocean interior may be reduced by the introduction of a harmonic viscosity A_h, which acts to damp EKE and also changes the strength and depth of the circulation cells.

In contrast, in the typically diabatic boundary regions, i.e. the surface boundary layer in the NL case and the surface and bottom boundary layers as well as the northern convective region in the flat case, both series expansions are alternating and increasing, which rules an adequate approximation by low order terms out, as previously discussed by Killworth (2001); McDougall and McIntosh (2001); Nurser and Lee (2004b). This intractable behaviour becomes more pronounced and severe in the hill case. There, physically inconsistent recirculation cells appear around the hill depth in the first order MOC, which are not effectively reduced by the inclusion of next higher order terms. On the contrary, the magnitude of the next higher order terms now even is increasing in the ocean interior (around hill depth and above topography around 500m depth), which further intensifies the recirculation cells and complicates the circulation patterns. This drawback of initially increasing series expansions does not disappear, if a harmonic viscosity A_h is introduced in the hill case. Consequently, an approximation of the ocean interior circulation by low order terms seems not to be possible in the hill case.

The increasing behaviour of both series expansions in certain regions of the ocean is the handicap which precludes a satisfying approximation of ψ^* or Ψ^* by low order terms. As

[13] That is, differences primarily appear in the regions where both series expansions are initially increasing - see two paragraphs further down.

an indicator of whether the series expansion of ψ^* is initially increasing or decreasing, we proposed the series number S, i.e. a dimensionless ratio relating the buoyancy perturbation with the mean isopycnal curvature scale. We find that in the diabatic boundary regions and at topographic depths, S represents a successful measure in our model experiments of whether the series expansion of ψ^* is initially increasing or not, while in the nearly adiabatic interior above topography, S is of reduced evidence. Since the increasing behaviour of the series expansion of Ψ^* is similar to the one of ψ^* in our model experiments, S applies in the same way to Ψ^*.

Consequently, in our model experiment which is equipped with a significant topographic feature and which hence represents the most realistic model setup, the approximations of the zonal-mean streamfunctions ψ^* and Ψ^* are most inappropriate. In order to interpret this problematic behaviour in the ocean interior in the hill case, we distinguish two regions, namely, on the one hand, the region around the hill depth and below, and, on the other hand, the interior region above topography. We interpret the problematic behaviour of the low order terms of ψ^* and Ψ^* in the former region as a zonally integrated boundary layer effect. As demonstrated in the NL case (section 3.1) and the flat case (section 3.2) and discussed in several previous studies (Killworth, 2001; McDougall and McIntosh, 2001; Nurser and Lee, 2004b), the approximations of ψ^* and Ψ^* typically break down in the horizontal boundary layers, which are generally characterised by diabatic processes and a vertically non-monotonic buoyancy field. While in the flat case these regions (surface, bottom) remain at fixed depth in the zonal dimension, the bottom boundary layer extends zonally over the hill-like topography in the hill case. More precisely, in the hill case we find significant values of the vertical diffusivity (not shown) indicating a small bottom boundary layer all along the bottom, but most pronounced at the hill depth. Hence, in the hill case, bottom boundary layer regions and interior parts are mixed up at topographic depths in the zonal integration carried out at fixed depth and along latitude circles. This mixture of boundary and interior regions precludes appropriate approximations of ψ^* and Ψ^* at topographic depths in a zonal-mean framework.

The second region of significant and increasing contributions in the lower order terms $\psi^*_{II}, \psi^*_{III}, ...$ and $\Psi^*_{II}, \Psi^*_{III}, ...$ is found above topography and centred around $y = 900$km. We do not relate the pure appearance of these contributions to the presence of topography, since they are also found, although weaker, in the flat case, even if the EKE is reduced by the introduction of A_h (see Fig. 2). But we ascribe the increasing behaviour of these contributions to the impact of topography on the zonal structure of the velocity and buoyancy fields: Typically, undulations emerge horizontally in the physical fields as an effect of topography (so-called standing eddies, Viebahn and Eden (2012)). In a zonal-mean framework of zonal integration along latitude circles, these undulations induce the amplification of the significant contributions above topography. However, the effect of standing eddies on the eddy streamfunctions vanishes, if the zonal integration paths are redefined so that the topographic influence is taken into account, or, more precisely, if the zonal integration is performed along time-mean isolines of buoyancy (which coincide with latitude circles in the flat case), as discussed by Viebahn and Eden (2012). If the zonal integration paths are defined this way, the zonal-mean eddy circulations of the flat case and the hill case

are more similar to each other. Hence, we expect that in a framework of zonal integration along time-mean isolines of buoyancy, an approximation of ψ^* and Ψ^* in the interior above topography would be possible again, just like in the flat case. In other words, we interpret the increasing behaviour above topography in the hill case not as a boundary layer effect in the zonal average, but as a topographic effect which might be circumvented by the appropriate choice of zonal integration paths. Moreover, also at topographic depths a reduction of the impact of the lower order terms might result from an appropriate redefinition of the zonal integration paths, but probably an effect of the boundary layer presence in the zonal average is inevitable.

A Outline of the residual-mean framework

The time-zonal-mean residual streamfunction $\psi_{res}(y,z)$ is defined as the meridional streamfunction which advects the Eulerian time-zonal-mean buoyancy $\overline{b}$. The time-zonal-mean buoyancy budget under steady state conditions is given by

$$\overline{v}\partial_y\overline{b} + \overline{w}\partial_z\overline{b} + L_x^{-1}(\partial_y(L_x\overline{v'b'}) + \partial_z(L_x\overline{w'b'})) = \overline{Q} \ , \tag{13}$$

where we used the decompositions[14] $b = \overline{b} + b'$, $v = \overline{v} + v'$ and $w = \overline{w} + w'$. The advection due to the time-zonal-mean velocity $(\overline{v}, \overline{w})$ is described by the time-zonal-mean Eulerian streamfunction Λ,

$$\partial_z\Lambda = -L_x\overline{v} \ , \qquad \partial_y\Lambda = L_x\overline{w} \ . \tag{14}$$

The eddy buoyancy flux $\mathbf{F}_b \equiv L_x(\overline{v'b'}, \overline{w'b'})$ may be decomposed into an additional advective part[15] $-\psi^*\underline{\nabla}\overline{b}$ (directed along the time-zonal-mean isopycnals) and a diffusive part (Andrews and McIntyre, 1976). The natural choice is to direct the diffusive part perpendicular to the advective part, i.e. along the buoyancy gradient $\nabla\overline{b}$ (Andrews and McIntyre, 1978b). This decomposition of the eddy buoyancy flux $\mathbf{F}_b$ is defined only up to an arbitrary rotational flux $\mathbf{F}_* = -\underline{\nabla}\theta$, given by the gauge potential θ, since $\mathbf{F}_b$ appears in the mean buoyancy equation (13) inside the divergence operator. In general, we have

$$\mathbf{F}_b = \kappa\nabla\overline{b} - \psi^*\underline{\nabla}\overline{b} - \underline{\nabla}\theta \ . \tag{15}$$

Using Eq. (15), we obtain for the buoyancy budget (13),

$$v_{res}\partial_y\overline{b} + w_{res}\partial_z\overline{b} = \overline{Q} - L_x^{-1}\nabla\cdot(\kappa\nabla\overline{b}) \ , \tag{16}$$

where the residual velocities $v_{res} = \overline{v} - L_x^{-1}\partial_z\psi^*$ and $w_{res} = \overline{w} + L_x^{-1}\partial_y\psi^*$ represent the total advection velocities of $\overline{b}$. Hence, the residual streamfunction ψ_{res} is given by

$$\psi_{res} = \Lambda + \psi^* \ . \tag{17}$$

[14] In a time-zonal-mean context, each quantity q generally may be decomposed into its temporal and zonal average $\overline{q}$ and its temporal and zonal deviation $q' \equiv q - \overline{q}$, i.e. $q = \overline{q} + q'$.

[15] The operator $\underline{\nabla}$ is defined as $\underline{\nabla} \equiv (-\partial_z, \partial_y)$.

ψ^* is the eddy streamfunction and defines the eddy-driven velocities

$$v^* = -L_x^{-1}\partial_z\psi^* \ , \qquad w^* = L_x^{-1}\partial_y\psi^* \ , \tag{18}$$

while the flux component $\kappa\nabla\overline{b}$ corresponds to a diffusive flux, and therefore the coefficient κ represents the diapycnal diffusivity induced by meso-scale eddies. Note that, since $\overline{b}$ does not retain the volumetric properties of the unaveraged buoyancy field b, the effect of eddies on $\overline{b}$ is inevitably both advective and diffusive (in contrast to isopycnal averaging, Nurser and Lee (2004b)).

The time-zonal-mean buoyancy $\overline{b}$ in Eq. (16) is forced by the small-scale diabatic forcing $\overline{Q}$ and the convergence of the meso-scale diffusive eddy flux $-L_x^{-1}\nabla\cdot(\kappa\nabla\overline{b})$. In order to ensure that, if there is no instantaneous diabatic buoyancy forcing Q, there is also no diabatic effects in the mean buoyancy budget, we have to consider the rotational eddy fluxes.

While the choice of θ has no influence on the mean buoyancy equation[16], it affects the eddy streamfunction ψ^* and the diapycnal diffusivity κ,

$$\psi^* = -\frac{(\mathbf{F}_b + \overline{\nabla}\theta)\cdot\overline{\nabla}\overline{b}}{|\nabla\overline{b}|^2} \ , \qquad \kappa = \frac{(\mathbf{F}_b + \overline{\nabla}\theta)\cdot\nabla\overline{b}}{|\nabla\overline{b}|^2} \ . \tag{19}$$

Further, the choice of the gauge potential θ affects the conservation equation of eddy variance $\overline{\phi_2} = \overline{b'b'}/2$, which is given by

$$\nabla\cdot\mathbf{F_2} = -\mathbf{F}_b\cdot\nabla\overline{b} + L_x\overline{b'Q'} \ , \tag{20}$$

where $\mathbf{F_2} = L_x(\overline{v}\overline{\phi_2} + \overline{v'\phi_2}, \overline{w}\overline{\phi_2} + \overline{w'\phi_2})$ represents the total variance flux, consisting of mean and turbulent variance advection. The term $\overline{b'Q'}$ denotes dissipation of variance and the term $-\mathbf{F}_b\cdot\nabla\overline{b} = -\kappa|\nabla\overline{b}|^2 + \overline{\nabla}\theta\cdot\nabla\overline{b}$ is a variance production term. The first term is positive for $\kappa > 0$ and hence a source of variance, while the second term can have both signs.

By considering the analog budgets of the higher order buoyancy moments, defined as $\overline{\phi_n} = \overline{b'^n}/n$ for order n, and applying decompositions of the corresponding fluxes $\mathbf{F}_n = L_x(\overline{v}\overline{\phi_n} + \overline{v'\phi_n}, \overline{w}\overline{\phi_n} + \overline{w'\phi_n})$ analog to Eq. (15), i.e. $\mathbf{F}_n = \kappa_n\nabla\overline{b} - \psi_n^*\overline{\nabla}\overline{b} - \overline{\nabla}\theta_n$, Eden et al. (2007) are able to show that, if the rotational flux potentials are specified as $n\theta_n = \psi_{n+1}^*$, then the turbulent diffusivity κ of Eq. (19) is given by the series

$$\kappa|\nabla\overline{b}|^2 = L_x\overline{b'Q'} - \mathcal{D}(L_x\overline{\phi_2 Q}) + \frac{1}{2}\mathcal{D}^2(L_x\overline{\phi_3 Q}) - \frac{1}{3!}\mathcal{D}^3(L_x\overline{\phi_4 Q}) + \ldots \ , \tag{21}$$

where $\mathcal{D}() \equiv \nabla\cdot\nabla\overline{b}|\nabla\overline{b}|^{-2}()$. In Eq. (21) κ is related to covariances between the small-scale forcing or mixing and buoyancy fluctuations. Hence, by specifying the gauge potentials

[16] More precisely, the sum of the additional eddy advection term $-\overline{\nabla}(\overline{\nabla}\theta\cdot\overline{\nabla}\overline{b}/|\nabla\overline{b}|^2)\cdot\nabla\overline{b}$ and the additional eddy diffusion term $\nabla\cdot(\overline{\nabla}\theta\cdot\nabla\overline{b}/|\nabla\overline{b}|^2\nabla\overline{b})$ identically vanishes.

as $n\theta_n = \psi^*_{n+1}$, there is no diapycnal turbulent mixing if there is no molecular mixing. The gauge condition $\theta = \psi^*_2$ states that the rotational flux potential is given by the flux of variance circulating along the contours of $\overline{b}$ (where ψ^*_2 is affected by the rotational flux potential of eddy variance θ_2).

Using $\psi^*_n |\nabla \overline{b}|^2 = -(\mathbf{F}_n + \underset{\neg}{\nabla}\theta_n) \cdot \underset{\neg}{\nabla}\overline{b}$ and the gauge condition $n\theta_n = \psi^*_{n+1}$, we obtain for the eddy streamfunction ψ^*,

$$\psi^* |\nabla \overline{b}| = -J_1 + \partial_m J_2 - \frac{1}{2}\partial^2_m J_3 + \frac{1}{3!}\partial^3_m J_4 - \ldots \ , \tag{22}$$

where $\partial_m() \equiv |\nabla\overline{b}|^{-1} \nabla\overline{b} \cdot \nabla |\nabla\overline{b}|^{-1}()$ and the $J_n \equiv \mathbf{F}_n \cdot \underset{\neg}{\nabla}\overline{b} |\nabla\overline{b}|^{-1}$ represent the along-isopycnal fluxes of the eddy buoyancy moments. The first order term in the expansion for ψ^* is identical to an eddy streamfunction of the transformed Eulerian mean (TEM) framework (Andrews and McIntyre, 1976, 1978b), i.e. the decomposition of $\mathbf{F}_b$ with $\underset{\neg}{\nabla}\theta \equiv 0$. The remainder of the expansion is due to the introduction of the rotational flux potential θ given by

$$\theta |\nabla \overline{b}| = -J_2 + \frac{1}{2}\partial_m J_3 - \frac{1}{3!}\partial^2_m J_4 + \ldots \ . \tag{23}$$

In the ocean interior, it typically holds $|\partial_y \overline{b}| \ll |\partial_z \overline{b}|$ and $|\overline{w}| \ll |\overline{v}|$ and we obtain

$$\psi^* \approx \frac{L_x \overline{v'b'}}{\partial_z \overline{b}} - \frac{1}{\partial_z \overline{b}} \partial_z \Big(\frac{L_x \overline{\phi_2 v}}{\partial_z \overline{b}} \Big) + \frac{1}{2} \frac{1}{\partial_z \overline{b}} \partial_z \Big(\frac{1}{\partial_z \overline{b}} \partial_z \Big(\frac{L_x \overline{\phi_3 v}}{\partial_z \overline{b}} \Big) \Big) - \ldots \tag{24}$$

$$\theta \approx \frac{L_x \overline{\phi_2 v}}{\partial_z \overline{b}} - \frac{1}{2} \frac{1}{\partial_z \overline{b}} \partial_z \Big(\frac{L_x \overline{\phi_3 v}}{\partial_z \overline{b}} \Big) + \frac{1}{3!} \frac{1}{\partial_z \overline{b}} \partial_z \Big(\frac{1}{\partial_z \overline{b}} \partial_z \Big(\frac{L_x \overline{\phi_4 v}}{\partial_z \overline{b}} \Big) \Big) - \ldots \tag{25}$$

$$\kappa \approx \frac{L_x \overline{b'Q'}}{(\partial_z \overline{b})^2} - \frac{1}{(\partial_z \overline{b})^2} \partial_z \Big(\frac{L_x \overline{\phi_2 Q}}{\partial_z \overline{b}} \Big) + \frac{1}{2} \frac{1}{(\partial_z \overline{b})^2} \partial_z \Big(\frac{1}{\partial_z \overline{b}} \partial_z \Big(\frac{L_x \overline{\phi_3 Q}}{\partial_z \overline{b}} \Big) \Big) - \ldots \tag{26}$$

B Third-order approximation of the quasi-Stokes streamfunction

We assume that the buoyancy field $b(x, y, z, t)$ is vertically strictly monotonic in the interior of the ocean. The instantaneous isopycnal b_a lies at an instantaneous height $z(x, y, b_a, t) = z_a(y, b_a) + z'_a(x, y, b_a, t)$, where z_a is the time-zonal-mean height of b_a and z'_a is the deviation from the time-zonal-mean, i.e. $\overline{z'_a} = 0$. The time-zonal-mean isopycnal streamfunction ψ_I is the temporally averaged zonal and depth integral of the velocity v, integrated below the isopycnal b_a. We may write

$$\psi_I(y, b_a) = -L_x \overline{\int_{bottom}^{z_a + z'_a} v \ dz} \ . \tag{27}$$

ψ_I may be transformed to Eulerian space by identifying each b_a with its mean height z_a. Therewith, the quasi-Stokes streamfunction Ψ^* is defined via the decomposition

$$-L_x \overline{\int_{bottom}^{z_a + z'_a} v \ dz} = \Lambda(y, z_a) + \Psi^*(y, z_a) \ , \tag{28}$$

that is,

$$\Psi^*(y, z_a) \equiv -L_x \overline{\int_{z_a}^{z_a+z'_a} v \; dz} \; , \tag{29}$$

and gives the transport of ψ_I related to the perturbation z'_a. Ψ^* is the eddy-induced streamfunction of ψ_I in Eulerian space[17]. Approximations of both z' and Ψ^* by Eulerian mean quantities may be obtained by expanding b and v in Taylor series (McDougall and McIntosh, 2001; Nurser and Lee, 2004b).

A vertical Taylor series of b centred at $z = z_a$ gives

$$b_a = b(z_a + z'_a) = b(z_a) + z'_a \partial_z b|_{z=z_a} + \frac{1}{2}(z'_a)^2 \partial_z^2 b|_{z=z_a} + \frac{1}{6}(z'_a)^3 \partial_z^3 b|_{z=z_a} + ...$$

Using the decomposition $b = \overline{b} + b'$, we obtain as terms up to third order in perturbation quantities (denoted by a)

$$\begin{aligned} b(z_a + z'_a) = \overline{b}(z_a) + b'(z_a) + z'_a \partial_z \overline{b}|_{z=z_a} + z'_a \partial_z b'|_{z=z_a} + \frac{1}{2}(z'_a)^2 \partial_z^2 \overline{b}|_{z=z_a} + \\ + \frac{1}{2}(z'_a)^2 \partial_z^2 b'|_{z=z_a} + \frac{1}{6}(z'_a)^3 \partial_z^3 \overline{b}|_{z=z_a} + O(a^4) \end{aligned}$$

Taking the temporal and zonal average of this equation yields

$$b_a = \overline{b}(z_a) + \overline{z'_a \partial_z b'|_{z=z_a}} + \frac{1}{2}\overline{(z'_a)^2} \partial_z^2 \overline{b}|_{z=z_a} + \frac{1}{2}\overline{(z'_a)^2 \partial_z^2 b'|_{z=z_a}} + \frac{1}{6}\overline{(z'_a)^3} \partial_z^3 \overline{b}|_{z=z_a} + O(a^4)$$

The difference of both equations gives

$$\begin{aligned} - z'_a \partial_z \overline{b}|_{z=z_a} \;\; = \;\; & b'(z_a) + z'_a \partial_z b'|_{z=z_a} - \overline{z'_a \partial_z b'|_{z=z_a}} + \frac{1}{2}((z'_a)^2 - \overline{(z'_a)^2}) \partial_z^2 \overline{b}|_{z=z_a} \\ & + \frac{1}{2}(z'_a)^2 \partial_z^2 b'|_{z=z_a} - \frac{1}{2}\overline{(z'_a)^2 \partial_z^2 b'|_{z=z_a}} + \frac{1}{6}((z'_a)^3 - \overline{(z'_a)^3}) \partial_z^3 \overline{b}|_{z=z_a} + O(a^4) \end{aligned}$$

From this last equation we obtain[18] a series expansion of z' (extending the approximation of McDougall and McIntosh (2001) about two orders),

$$\begin{aligned} z' \;\; = \;\; & -\frac{b'}{\partial_z \overline{b}} + \frac{1}{\partial_z \overline{b}} \partial_z \left(\frac{\phi_2}{\partial_z \overline{b}} \right) - \frac{L_x^{-1}}{\partial_z \overline{b}} \partial_z \left(\frac{L_x \overline{\phi_2}}{\partial_z \overline{b}} \right) + \frac{L_x^{-1}}{\partial_z \overline{b}} \partial_z \left(\frac{b'}{\partial_z \overline{b}} \right) \partial_z \left(\frac{L_x \overline{\phi_2}}{\partial_z \overline{b}} \right) - \\ & - \frac{1}{2} \frac{1}{\partial_z \overline{b}} \partial_z \left(\frac{1}{\partial_z \overline{b}} \partial_z \left(\frac{\phi_3}{\partial_z \overline{b}} \right) \right) + \frac{1}{2} \frac{L_x^{-1}}{\partial_z \overline{b}} \partial_z \left(\frac{1}{\partial_z \overline{b}} \partial_z \left(\frac{L_x \overline{\phi_3}}{\partial_z \overline{b}} \right) \right) + O(b'^4) \end{aligned} \tag{30}$$

[17] In Viebahn and Eden (2012) the corresponding decomposition is defined in an isopycnal framework.

[18] Note that if the topography varies vertically, then the zonal average and the vertical derivative do not commute due to the depth-dependent factor L_x.

By expanding v in a vertical Taylor series, we obtain for the quasi-Stokes streamfunction Ψ^*,

$$\begin{aligned}
\Psi^* &= -L_x\Big(\overline{v(z_a)z'_a} + \frac{1}{2}\overline{(z'_a)^2\partial_z v|_{z=z_a}} + \frac{1}{6}\overline{(z'_a)^3\partial_z^2 v|_{z=z_a}} + ...\Big) \\
&= -L_x\Big(\overline{v'(z_a)z'_a} + \frac{1}{2}\overline{(z'_a)^2}\partial_z\overline{v}|_{z=z_a} + \frac{1}{2}\overline{(z'_a)^2\partial_z v'|_{z=z_a}} + \\
&\qquad + \frac{1}{6}\overline{(z'_a)^3}\partial_z^2\overline{v}|_{z=z_a} + \frac{1}{6}\overline{(z'_a)^3\partial_z^2 v'|_{z=z_a}} + ...\Big) \ ,
\end{aligned} \tag{31}$$

where we used the decomposition $v = \overline{v} + v'$. Using Eq. (30) in Eq. (31), we obtain up to third order in perturbation quantities (extending the approximation of McDougall and McIntosh (2001) about one order)

$$\Psi^* = \Psi_1^* + \Psi_2^* + \Psi_3^* + O(a^4) \ , \tag{32}$$

where

$$\Psi_1^* \equiv 0 \tag{33}$$

$$\Psi_2^* = \frac{L_x\overline{b'v'}}{\partial_z\overline{b}} - \frac{L_x\overline{\phi_2}\partial_z\overline{v}}{(\partial_z\overline{b})^2} \tag{34}$$

$$\Psi_3^* = -\frac{1}{\partial_z\overline{b}}\partial_z\Big(\frac{L_x\overline{\phi_2 v'}}{\partial_z\overline{b}}\Big) + \frac{1}{2}\frac{\partial_z\overline{v}}{(\partial_z\overline{b})^2}\partial_z\Big(\frac{L_x\overline{\phi_3}}{\partial_z\overline{b}}\Big) + \frac{1}{2}\frac{1}{\partial_z\overline{b}}\partial_z\Big(\frac{L_x\overline{\phi_3}\partial_z\overline{v}}{(\partial_z\overline{b})^2}\Big) \tag{35}$$

In order to make the relation between Ψ^* and the residual-mean eddy streamfunction ψ^* (see (24)) more obvious, we arrange the expansion of Ψ^* in orders of buoyancy perturbations b' (extending the approximation of Nurser and Lee (2004b) and of Eq. (32)),

$$\Psi^* = \Psi_I^* + \Psi_{II}^* + \Psi_{III}^* + O(b'^4) \ , \tag{36}$$

where

$$\Psi_I^* = \frac{L_x\overline{b'v'}}{\partial_z\overline{b}} = \psi_I^* \tag{37}$$

$$\Psi_{II}^* = -\frac{1}{\partial_z\overline{b}}\partial_z\Big(\frac{L_x\overline{\phi_2 v}}{\partial_z\overline{b}}\Big) + \frac{\overline{v}}{\partial_z\overline{b}}\partial_z\Big(\frac{L_x\overline{\phi_2}}{\partial_z\overline{b}}\Big) = \psi_{II}^* + \psi_{\Delta II}^* \tag{38}$$

$$\begin{aligned}
\Psi_{III}^* &= \frac{1}{2}\frac{1}{\partial_z\overline{b}}\partial_z\Big(\frac{1}{\partial_z\overline{b}}\partial_z\Big(\frac{L_x\overline{\phi_3 v}}{\partial_z\overline{b}}\Big)\Big) - \\
&\quad -\frac{1}{2}\frac{\overline{v}}{\partial_z\overline{b}}\partial_z\Big(\frac{1}{\partial_z\overline{b}}\partial_z\Big(\frac{L_x\overline{\phi_3}}{\partial_z\overline{b}}\Big)\Big) - \frac{L_x^{-1}}{\partial_z\overline{b}}\partial_z\Big(\frac{L_x\overline{\phi_2}}{\partial_z\overline{b}}\Big)\partial_z\Big(\frac{L_x\overline{v'b'}}{\partial_z\overline{b}}\Big) \\
&= \psi_{III}^* + \psi_{\Delta IIIa}^* + \psi_{\Delta IIIb}^*
\end{aligned} \tag{39}$$

References

Andrews, D. G. and M. E. McIntyre, 1976: Planetary waves in horizontal and vertical shear: The generalized Eliassen-Palm relation and the zonal mean accelaration. *J. Atmos. Sci.*, **33**, 2031–2048.

Andrews, D. G. and M. E. McIntyre, 1978a: An exact theory of nonlinear waves on a Lagrangian-mean flow. *J. Fluid Mech.*, **89**, 609–646.

Andrews, D. G. and M. E. McIntyre, 1978b: Generalized Eliassen-Palm and Charney-Drazin theorems for waves on axisymmetric mean flows in compressible atmosphere. *J. Atmos. Sci.*, **35**, 175–185.

de Szoeke, R. A. and A. F. Bennett, 1993: Microstructure fluxes across density surfaces. *J. Phys. Oceanogr.*, **23**, 2254–2264.

Döös, K. and D. J. Webb, 1994: The Deacon cell and the other meridional cells of the Southern Ocean. *J. Phys. Oceanogr.*, **24**, 429–442.

Eden, C., R. J. Greatbatch, and D. Olbers, 2007: Interpreting eddy fluxes. *J. Phys. Oceanogr.*, **37**, 1282–1296.

Eden, C., D. Olbers, and R. J. Greatbatch, 2009: A generalized Osborn-Cox relation. *J. Fluid Mech.*, **632**, 457–474.

Killworth, P. D., 2001: Boundary conditions on quasi-Stokes velocities in parameterizations. *J. Phys. Oceanogr.*, **31**, 1132–1155.

Marshall, J. and T. Radko, 2003: Residual-mean solutions for the Antarctic Circumpolar Current and its associated overturning circulation. *J. Phys. Oceanogr.*, **33**, 2341–2354.

McDougall, T. J. and P. C. McIntosh, 1996: The temporal-residual-mean velocity. Part I: Derivation and the scalar conservation equations. *J. Phys. Oceanogr.*, **26**, 2653–2665.

McDougall, T. J. and P. C. McIntosh, 2001: The temporal-residual-mean velocity. Part II: Isopycnal interpretation and the tracer and momentum equations. *J. Phys. Oceanogr.*, **31**, 1222–1246.

Medvedev, A. S. and R. J. Greatbatch, 2004: On advection and diffusion in the mesosphere and lower thermosphere: The role of rotational fluxes. *J. Geophys. Res.*, **109**, D07104 doi:10.1029/2003JD003931.

Nurser, A. J. G. and M.-M. Lee, 2004a: Isopycnal averaging at constant height. Part I: The formulation and a case study. *J. Phys. Oceanogr.*, **34**, 2721–2739.

Nurser, A. J. G. and M.-M. Lee, 2004b: Isopycnal averaging at constant height. Part II: Relating to the residual streamfunction in Eulerian spa ce. *J. Phys. Oceanogr.*, **34**, 2740–2755.

Viebahn, J. and C. Eden, 2010: Towards the impact of eddies on the response of the Southern Ocean to climate change. *Ocean Modell.*, **34**, 150–165.

Viebahn, J. and C. Eden, 2012: Standing eddies in the meridional overturning circulation. *J. Phys. Oceanogr.*, pp. doi:10.1175/JPO–D–11–087.1.

Walin, G., 1982: On the relation between sea-surface heat flow and thermal circulation in the ocean. *Tellus*, **34**, 187–195.

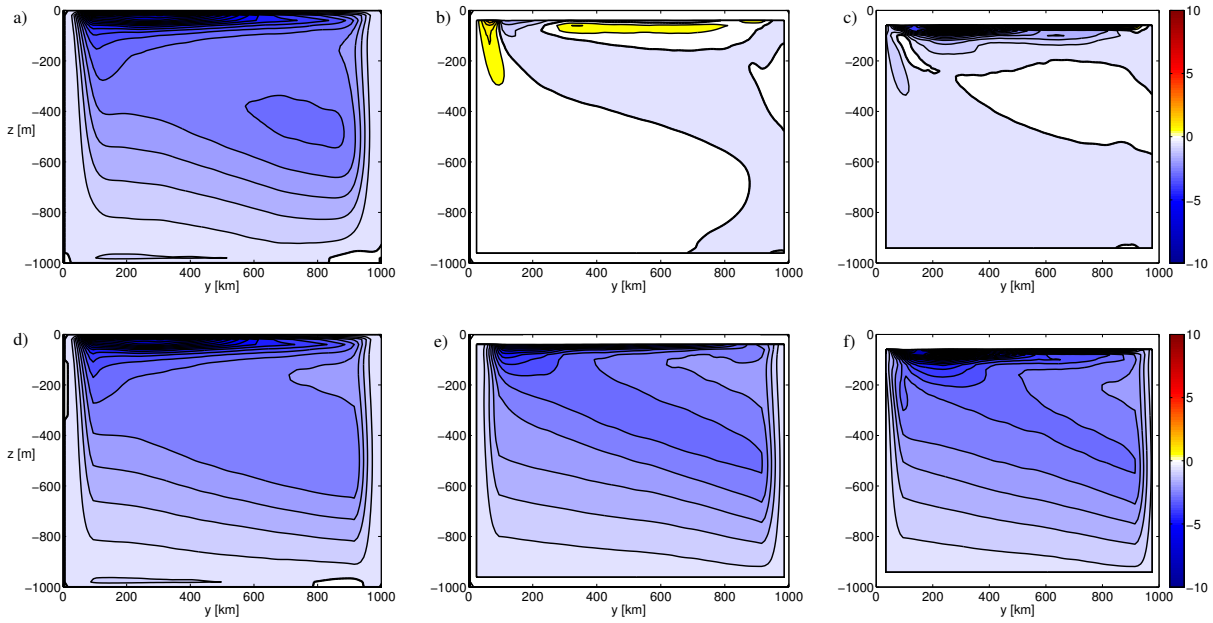

Figure 1: The first three terms of the series expansion of ψ^* for the NL case: $\psi^*_I \equiv -J_1/|\nabla\bar{b}|$ (a), $\psi^*_{II} \equiv \partial_m J_2/|\nabla\bar{b}|$ (b), $\psi^*_{III} \equiv -\frac{1}{2}\partial^2_m J_3/|\nabla\bar{b}|$ (c) and the corresponding residual streamfunctions including terms of ψ^* up to the first (d), second (e), third (f) order. The contour interval is 0.5Sv and zero lines are thick.

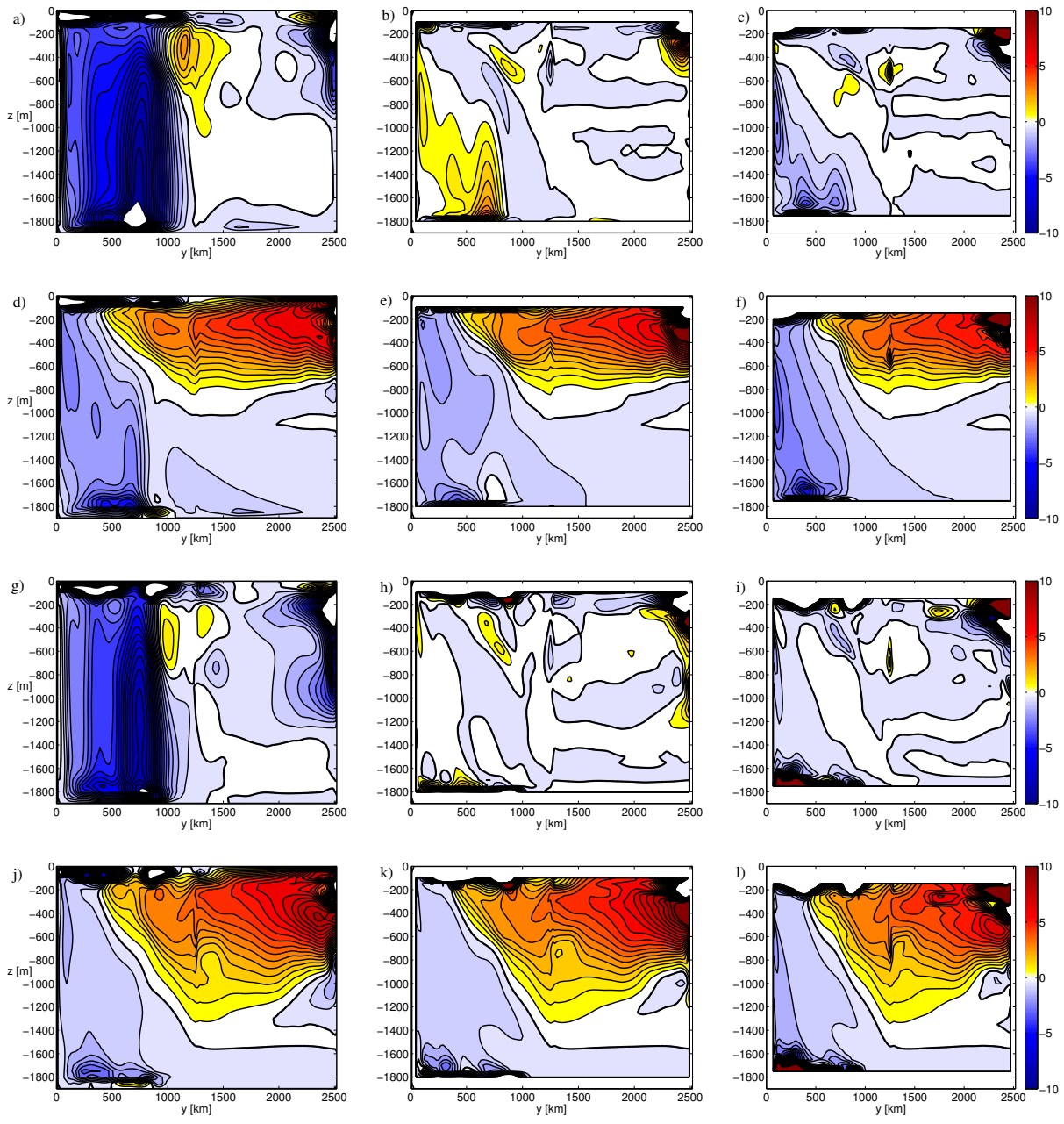

Figure 2: The first three terms of the series expansion of ψ^* for the flat case: ψ^*_I (a), ψ^*_{II} (b), ψ^*_{III} (c) and the corresponding residual streamfunctions including terms of ψ^* up to the first (d), second (e), third (f) order. (g-i) and (j-l) show the same quantities, but for the flat case experiment including a harmonic viscosity of $A_h = 2000\mathrm{m}^2\mathrm{s}^{-1}$. The contour interval is 0.5Sv and zero lines are thick.

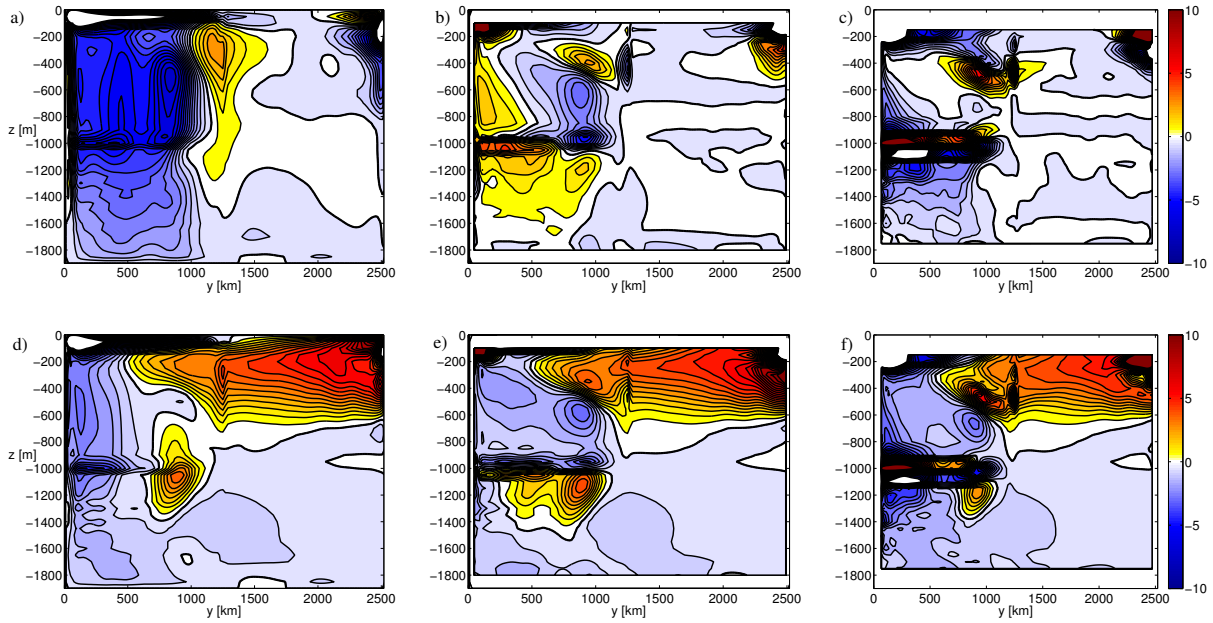

Figure 3: The first three terms of the series expansion of ψ^* for the hill case: ψ^*_I (a), ψ^*_{II} (b), ψ^*_{III} (c) and the corresponding residual streamfunctions including terms of ψ^* up to the first (d), second (e), third (f) order. The contour interval is 0.5Sv and zero lines are thick.

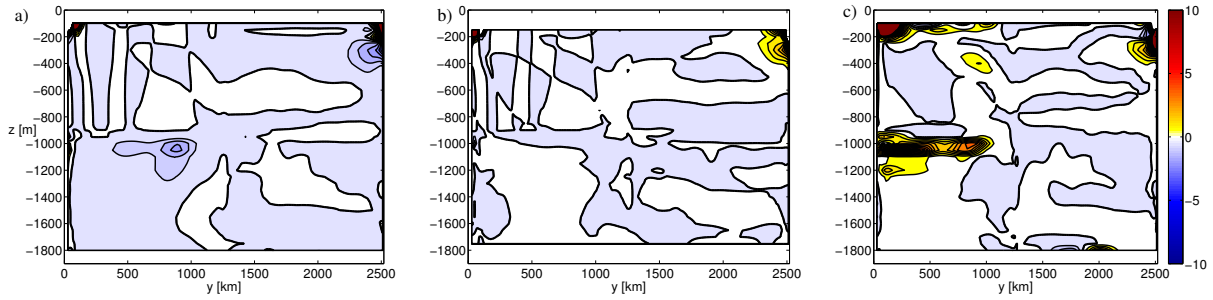

Figure 4: $\psi^*_{\Delta II}$ (a), $\psi^*_{\Delta IIIa}$ (b) and $\psi^*_{\Delta IIIb}$ (c) for the hill case. The contour interval is 0.5Sv and zero lines are thick.

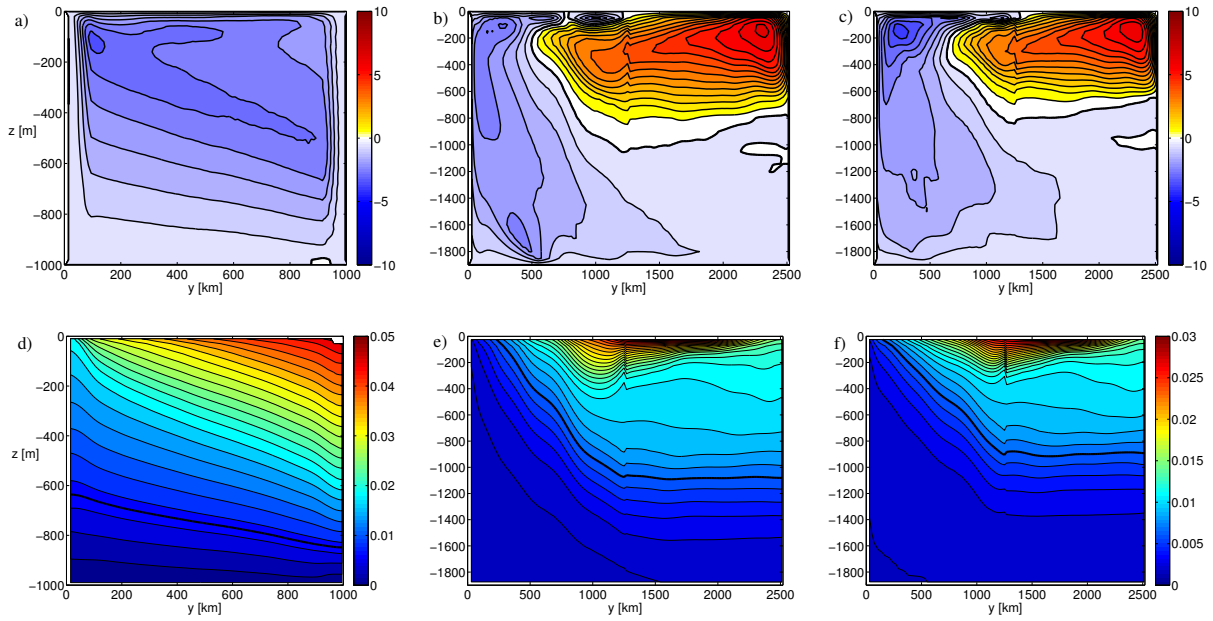

Figure 5: Isopycnal streamfunction transformed to depth coordinates via the mean height of isopycnals (Nurser and Lee, 2004a) for the NL case (a), flat case (b) and hill case (c). The contour interval is 0.5Sv and zero lines are thick. Below are shown the corresponding mean isopycnals (i.e. the isopycnally averaged buoyancy distributions), where in the NL case (d) the contour interval is $0.002\mathrm{m/s}^2$, while in the flat case (e) and the hill case (f) the contour interval is $0.001\mathrm{m/s}^2$. In all three cases the $0.007\mathrm{m/s}^2$ line is thick.

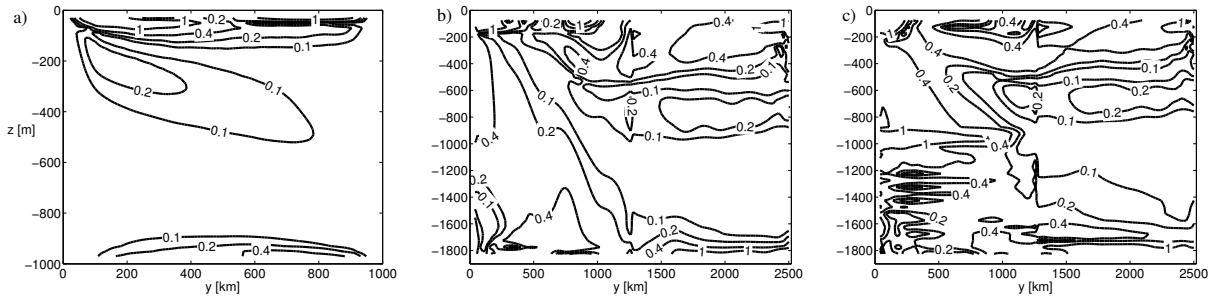

Figure 6: Series number S for the NL case (a), the flat case (b) and the hill case (c). Contour lines are 0.1, 0.2, 0.4 and 1.